High-temperature measurement using fiber Bragg grating sensor accompanied by a low-cost detection system

Article *in* Journal of Applied Remote Sensing · May 2015

DOI: 10.1117/1.JRS.9.094098

CITATIONS
19

READS
724

6 authors, including:

Venkata Reddy Mamidi
Vignan Institute of Technology & Science, Hyderabad
21 PUBLICATIONS **336** CITATIONS
SEE PROFILE

Kamineni Srimannarayana
National Institute of Technology, Warangal
16 PUBLICATIONS **317** CITATIONS
SEE PROFILE

Lakshminarayana Sai Prasad Ravinuthala
National Institute of Technology, Warangal
10 PUBLICATIONS **113** CITATIONS
SEE PROFILE

Tumu Venkatappa Rao
National Institute of Technology, Warangal
70 PUBLICATIONS **940** CITATIONS
SEE PROFILE

Journal of
Applied Remote Sensing

RemoteSensing.SPIEDigitalLibrary.org

High-temperature measurement using fiber Bragg grating sensor accompanied by a low-cost detection system

Venkata Reddy Mamidi
Srimannarayana Kamineni
L. N. Sai Prasad Ravinuthala
Manohar Martha
Sai Shankar Madhuvarasu
Venkatappa Rao Thumu

SPIE.

High-temperature measurement using fiber Bragg grating sensor accompanied by a low-cost detection system

Venkata Reddy Mamidi,* Srimannarayana Kamineni, L. N. Sai Prasad Ravinuthala, Manohar Martha, Sai Shankar Madhuvarasu, and Venkatappa Rao Thumu
National Institute of Technology, Department of Physics, Warangal 506004, India

Abstract. A fiber Bragg grating (FBG)–based high-temperature sensor accompanied by a low-cost interrogation scheme with liquid-crystal display (LCD) has been designed, developed, and tested. The sensor probe is configured by encapsulating a femtosecond laser drawn FBG with an aluminum nitride capillary tube, and is used to measure the temperature from 20°C to 650°C. The interrogation system consists of a long period fiber grating, two photodiodes, a 2-channel transimpedance amplifier, and a field-programmable gate array with an LCD. It displays the temperature directly in °C with a resolution of 1°C. The sensor output is found to be linear with coefficient of 0.999, and independent of source power fluctuations. The results showed that the sensor has good accuracy with a negligible error bar of ±1.23%. [DOI: 10.1117/1.JRS.9.094098]

Keywords: temperature measurement; FBG sensor; sensor display; fiber optic temperature sensor; long-period grating.

Paper 15018 received Jan. 7, 2015; accepted for publication Apr. 14, 2015; published online May 13, 2015.

1 Introduction

Temperature measurement encompasses a wide variety of needs and applications. To meet these requirements, industry must develop a large number of sensors and devices.[1] In order to obtain accurate, three-dimensional spatial information regarding the temperature distribution with real-time monitoring, fiber Bragg gratings (FBGs) have been adapted as intelligent sensing elements.[2,3] They have achieved tremendous growth in sensing, telecommunications, and optical switching applications owing to all the advantages of fiber optics such as compactness, light weight, immunity to electromagnetic interference, high reliability, fast response, high sensitivity, and capabilities of distributed sensing, multiplexing, and multiparameters.[4,5]

FBGs are compact intrinsic optical devices constructed in a small segment of an optical fiber. They are obtained by creating periodic variations in the refractive index of the core of a photosensitive optical fiber from exposure to an intense ultraviolet interference pattern.[6] When an FBG is illuminated by a broadband light source, it reflects a particular narrow band of wavelength called the Bragg wavelength and transmits all others. The Bragg wavelength is expressed as $\lambda_B = 2n_{\text{eff}}\,\Lambda$, where n_{eff} is the effective index of refraction of the fiber core at free space center wavelength, and Λ is the grating period.[7] Even a minute change in either of the aforementioned parameters due to external perturbation causes a considerable wavelength shift, and this wavelength shift itself can be the measure of the external perturbation.[8] In this way, FBGs are capable of measuring a wide range of parameters such as temperature, strain/stress, pressure, curvature, vibration, displacement, electrical current, voltage, load, and ambient refractive index.[9,10] Over the past two decades, FBGs have seen increased acceptance in a variety of sensing applications

*Address all correspondence to: Venkata Reddy Mamidi, E-mail: mamidivenkatreddy@gmail.com
1931-3195/2015/$25.00

such as health monitoring of civil, aerospace, marine, oil and gas, composites, and smart structures.[11,12]

The principle of the FBG-based temperature sensor involves the measurement of shift in Bragg wavelength, while strain on FBG remains unchanged.[13] The wavelength shift for a temperature change (ΔT) is given as

$$\Delta\lambda_{B(t)} = \lambda_B(\alpha + \xi)\Delta T, \tag{1}$$

where $\alpha = (1/\Lambda)(\partial\Lambda/\partial T)$ is the thermal expansion coefficient of the fiber and $\xi = (1/n_{\text{eff}})(\partial n_{\text{eff}}/\partial T)$ represents thermo-optic coefficient.[14,15] Due to the fragile nature of FBGs, it is therefore necessary to encapsulate them appropriately to enable them to survive in harsh environments.[8,16] Moreover, the use of an optical spectrum analyzer (OSA) to readout the wavelength information from FBG increases the size and cost of the system significantly, and also limits the scanning speed.[16] Therefore, a compact and low-cost interrogation system with display is to be developed for successful implementation of the technology in engineering applications.

This article gives a detailed description about the design of a compact FBG-based sensor system that includes a sensor probe, an interrogation scheme, and a digital display to measure temperatures of up to 650°C.

2 Design and Operation

Figure 1 shows a schematic of the sensor system that includes a fiber-coupled broadband superluminescent diode light source (BBS, 1525–1565 nm), an optical circulator, an FBG sensor probe, 1×2 optical coupler, an athermalized long-period fiber grating (LPG), two fiber pigtailed photodiodes (InGaAs PIN photodiodes, $Vr = 5$ V @ 25°C) (PD1, PD2), a 2-channel transimpedance amplifier (TIA) circuit, and a field-programmable gate array (FPGA) circuitry with a dual analog-to-digital converter (D-ADC), signal processing unit, and liquid-crystal display (LCD).

2.1 *Fiber Bragg Grating Sensor Probe*

The sensor probe is configured by encapsulating a femtosecond-laser-drawn FBG of specifications given in Table 1 with an aluminum nitride (ceramic) capillary tube. The tube measures 20 cm in length and 2 mm, 3.2 mm in inner and outer diameters, respectively. Due to the brittle nature of the ceramic tube, the sensor probe is safeguarded appropriately by using a stainless steel tube. To avoid the effect of the stainless steel tube on the response time of the sensor, aspiratory holes are provided on it at the location of the FBG. The FBG inside the probe is fixed such that it does not receive any strain impact either by the ceramic tube or by the stainless steel tube. The sensor probe is then inserted in a steel rod by making use of a brass holder and is

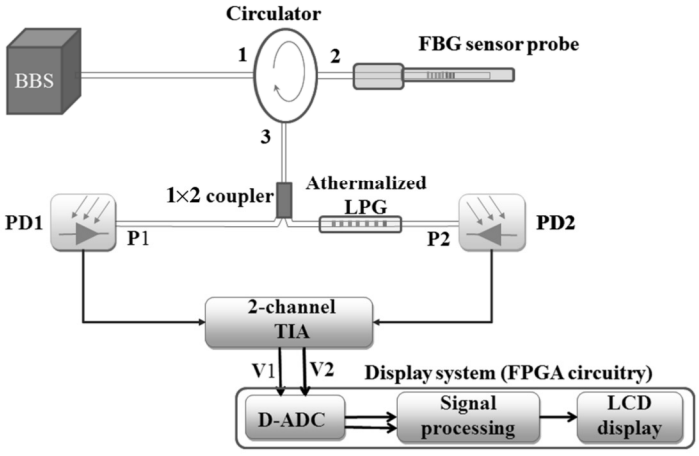

Fig. 1 Schematic of the sensor system.

Table 1 Specifications of fiber Bragg grating (FBG) and long-period fiber grating (LPG).

	FBG	LPG
Fiber type	SMF 28	SMF 28
Center wavelength (@ 20°C)	1537.57 nm	1550.32 nm
Side mode suppression ratio/peak attenuation	~15.95 dB	~28.2 dB
FWHM	~0.29 nm	~22.1 nm
Length	5 mm	20 mm
Linear edge region of LPG (at raising edge)	NA	1535.50–1545.0 nm

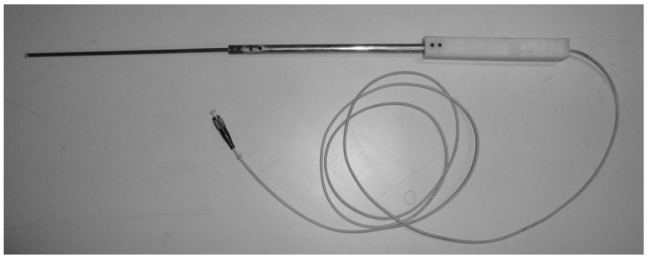

Fig. 2 Photograph of fiber Bragg grating (FBG) sensor probe.

sealed with a high-temperature adhesive. A heat-resisting handle comprised of Nylon is employed for easy and safe handling from thermal hazards, and an optical fiber patch card with an FC/PC connector facilitates the sensor head to connect with the measurement unit. Figure 2 shows a photograph of the sensor probe with a novel encapsulation technique permitting an easy and secure use of FBG at high temperature, which was already presented in our previous work.[8] When the FBG sensor is subjected to temperature, the reflected Bragg wavelength is linearly red-shifted.

2.2 *1 × 2 Optical Coupler*

It is a 3-dB coupler, which distributes the light signal (power) from the FBG equally between two fiber arms. One of these two arms couples the power P1 to PD1 directly, whereas the other couples a modulated power P2 to PD2 through an athermalized LPG.

2.3 *Athermalized Long-Period Fiber Grating*

LPGs are the second class of fiber gratings with a much longer period than that of FBG. They are sensitive to a range of measurands, particularly strain, temperature, bend radius, and the

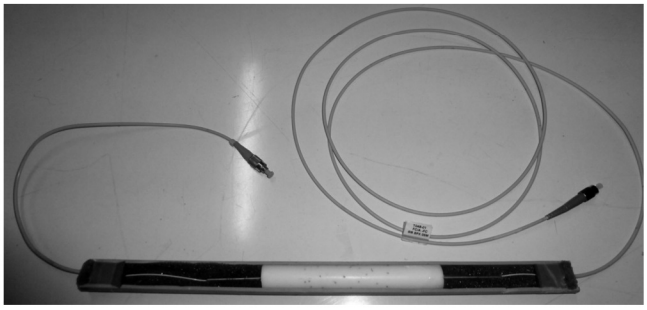

Fig. 3 Photograph of athermalized long-period fiber grating (LPG).

refractive index of the surrounding media, and thus can be used as sensing elements. Also a particular characteristic spectral range in the attenuation band of the LPG acts as an optical edge filter for interrogation of FBG sensors by converting the wavelength information of the FBG into its equivalent intensity information ($P2$). In order to make this interrogation scheme effective, the LPG is to be athermalized such that the attenuation band yields a unique intensity response to the given wavelength signal. Here, a CO_2 laser drawn LPG of specifications given in Table 1 is athermalized with a novel encapsulating technique by means of creating the opposite effect from temperature-induced strain, achieved by encapsulating it appropriately in a specially designed Teflon tube. A photograph of the athermalized LPG is shown in Fig. 3, which was explained in detail in our previous work.[17]

2.4 *Transimpedance Amplifier with Signal Conditioning Circuitry*

A multifunctional 2-channel amplifier board (TWLUX TW30-series) is developed and used for this experiment. It has two independent amplifier channels with adjustable gain. By using jumpers one can select the amplifier type (voltage or transimpedance amplifier). The board provides a current gain ranging over $10^4 - 10^7$ V/A with a range of output voltage from 0 to 3.4 V.[18] Here, the two fiber pigtailed photodiodes PD1 and PD2 are directly plugged into sockets. The output voltage signals are available on screw terminals of outputs 1 and 2, respectively. The voltage signals from TIA are to be modulated further as per the requirement of ADC for further processing. Hence, the circuit is extended by a simple voltage adder/subtractor in each of the channels. After signal conditioning, the two output voltage signals corresponding to P1 and P2 are termed V1 and V2, respectively.

2.5 *Display System*

A Spartan 3-E FPGA starter kit is used to convert the voltage signals from TIA into a visual display. It mainly consists of a D-ADC, signal processing unit, and an LCD display. As shown in Fig. 4, the board consists of a programmable preamplifier, a serial 14-bit D-ADC, software units for linearization and processing of ADC outputs, address generation and data memory, and a 2-line, 16-character LCD display. All these modules are integrated and fused into the FPGA, and programmed by very high-speed integrated circuits hardware description language (VHDL) coding.

The preamplifier (LTC6912-1) had two independent inverting amplifiers with programmable gain. The purpose of this amplifier is to scale the incoming analog signal to a full range of ADC input voltage scale so that the complete conversion range of the ADC with maximum number of samples can be utilized. Its entire functioning depends on interface signal through the VHDL program.

The D-ADC (LTC 1407A-1) converts analog input ranging over 0.4–2.9 V (window of 2.5 V) to digital output of 14 bit with a resolution of 0.0002 V. But according to the ADC data sheet, best use of 10 bits only is allowed due to integral linearity error. Therefore, the

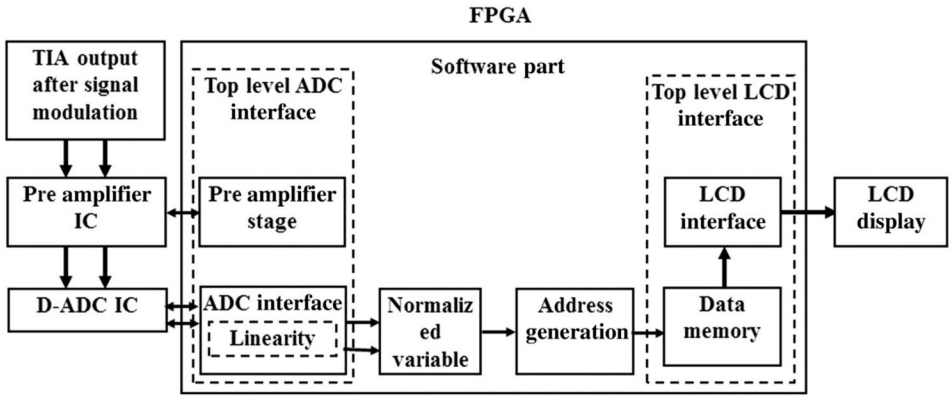

Fig. 4 Block diagram of field programmable gate array (FPGA) board.

practical voltage resolution is limited to about 0.0025 V. In the present application, the dynamic range of input voltage is 0.4–2.7 V and the temperature to be measured by the sensor is 20°C–650°C. Hence, the resolution is limited to 0.7°C (~1°C). It simultaneously digitalizes both the input voltage signals.

Linearization of the ADC output is necessary to make the digital output consistent with the input voltage. The digital output of ADC starts at the binary code of 8191 with the input voltage of 0.4 V and is reduced up to zero. Then the output takes a step to 16,383 and comes down to 8192. To obtain a linear response with single slope, a simple algorithm "if MSB of 14 bit ADC is zero, then subtract the ADC output from 8192, else if the MSB is '1' then subtract the ADC value from 24576" is used. Now it is very easy to convert these digital values into the measurand of interest.

The normalized output of the two digital signals corresponding to V1 and V2 is defined as

$$X = 2.9 \times \frac{(\mathrm{V1} - \mathrm{V2})}{\mathrm{V1}}, \tag{2}$$

where 2.9 is the maximum input voltage of ADC, which avoids the effect of source power fluctuations on temperature measurement.

The address generation block is meant to generate an address for the data which is stored in data memory and is to be displayed. It generates a 10-bit address with ADC digital output, and the data stored in this address is displayed on the LCD screen. Here, the address generation formula is defined as a function of the normalized output as

$$\mathrm{Address} = 20 + (X - 88) \times \frac{934}{630}. \tag{3}$$

The address generated from the aforementioned equation is a binary code equivalent to the corresponding temperature.

Data memory consists of all the data to be displayed on LCD, in terms of character-code. For this experiment, the data to be displayed is the temperature readings; 20, 21, 22...650°C. Hence, each address location in data memory is stored with a data of character-code of the corresponding temperature reading. For example, a character-code of 80 is specified with an address of 0001010000 (= 80).

The LCD displays the data that are stored in the data memory and addressed by the address generation block. The Spartan-3E starter kit board prominently featured a 2-line, 16-character LCD.

2.6 *Sensor Assembly*

The photograph of the sensor assembly is shown in Fig. 5. The light from the BBS illuminates the FBG in sensor probe. The reflected power of the Bragg resonance wavelength is split into two

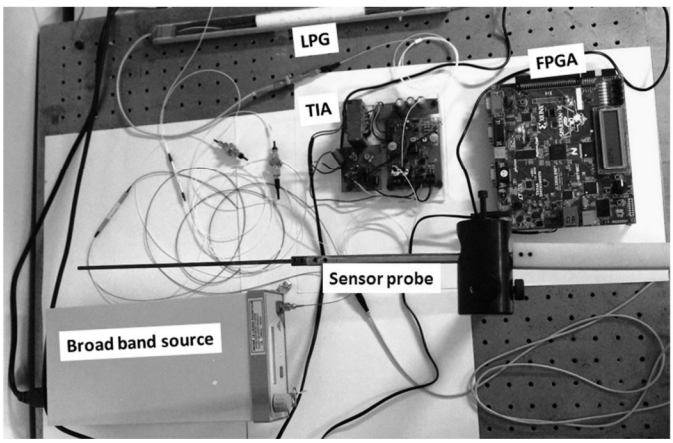

Fig. 5 Photograph of the sensor assembly.

single-mode fibers. One is directly coupled to PD1, whereas the other is connected to PD2 after being modulated by the LPG edge filter. Now the electrical current signals from PD1 and PD2 are converted into their equivalent voltage signals using the TIA. After signal conditioning, both the voltage signals are given to the FPGA starter kit to measure and display the temperature reading on the LCD screen.

3 Experimental Details

The sensor probe is inserted into a tubular furnace and is subjected to a temperature ranging between 20°C and 650°C. For every 5°C temperature change, the Bragg wavelength and peak power of FBG reflected spectrum are recorded, while heating as well as cooling. Later the reflected power of FBG is split into two fiber arms, one with reference to power P1 and another with LPG modulated power P2. The optical power signals (P1 and P2) that are captured by PD1 and PD2, respectively, are converted into voltage signals using 2-channel TIA with signal conditioning circuitry. Both the voltage signals V1 and V2 are measured using digital multimeters over the span of applied temperature. By repeatedly performing the experiment,

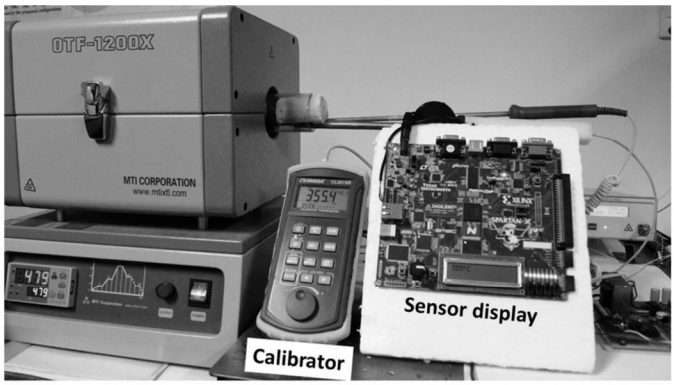

Fig. 6 Photograph of the experimental setup.

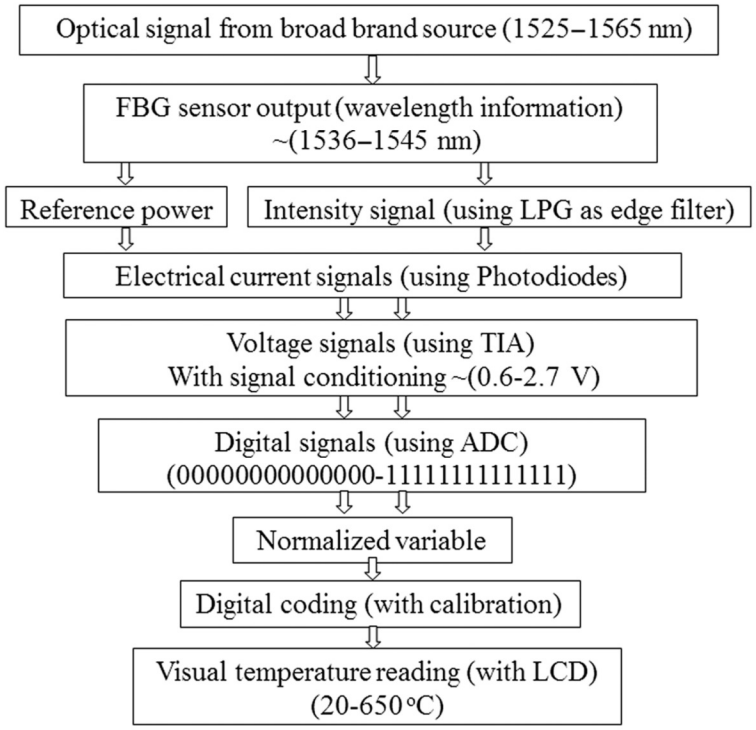

Fig. 7 Signal-flow chart of the sensor system.

the sensor is calibrated with a temperature calibrator. Furthermore, the sensor system is integrated with the display system to normalize and display the output that corresponds to the applied temperature. Figure 6 shows a photograph of the experimental setup of the sensor system. A signal-flow chart of the sensor system from FBG to the digital display is given in Fig. 7.

4 Results and Discussion

4.1 *Wavelength and Power Modulation*

Figure 8 shows the temperature response of the sensor probe in terms of Bragg wavelength and peak power (intensity). The sensor probe has shown fine temperature characteristics in both wavelength as well as intensity modulations. The shift (redshift) in Bragg wavelength is found to be 13.3 pm/°C with a linear coefficient of 0.999, whereas the intensity modulation of FBG signal due to LPG edge filter is found to be −1.81 nW/°C with a linear coefficient

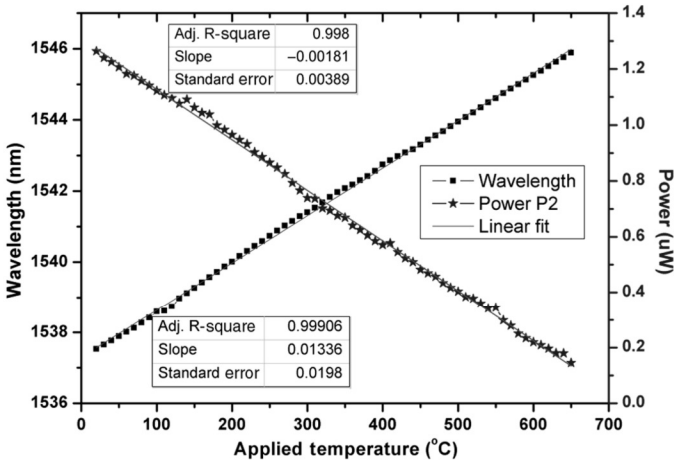

Fig. 8 Temperature response of the sensor probe after modulation by the LPG edge filter.

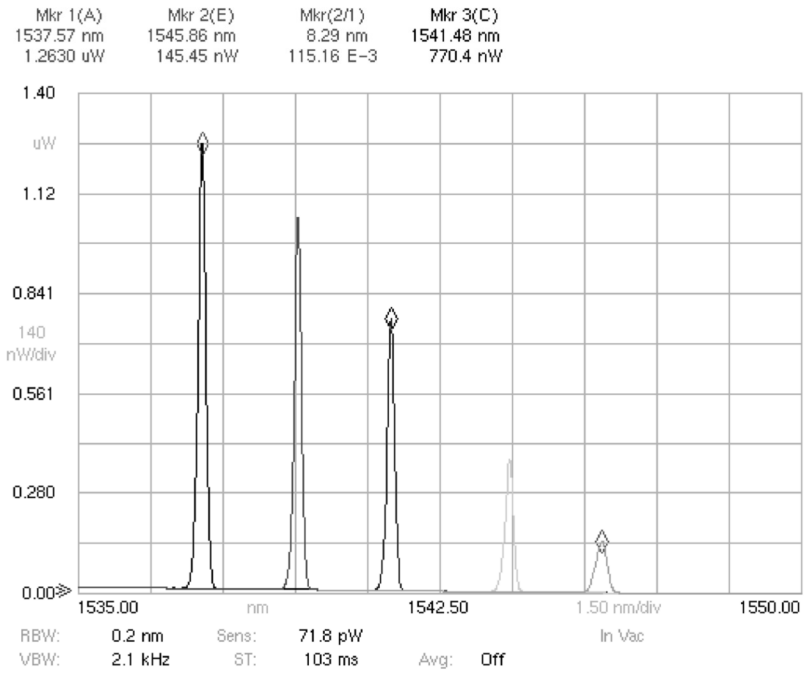

Fig. 9 Spectral response of FBG sensor over the span of temperature 20°C–650°C.

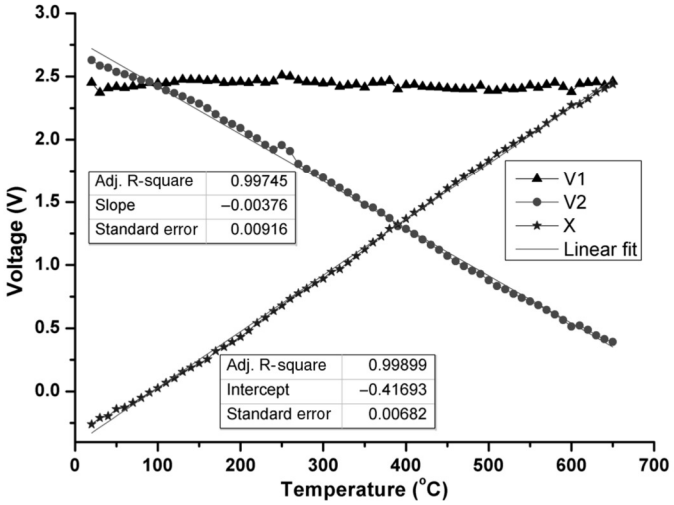

Fig. 10 Temperature response of the sensor in terms of electrical voltage.

of 0.998. Figure 9 shows the spectral response of the FBG sensor after being modulated by the LPG edge filter, over the span of temperature 20°C–650°C. The conversion of wavelength information into its equivalent intensity signal rendered the system low-cost by enabling the sensor output to be captured using a simple PD.

4.2 *Electrical Voltage Signal*

The electrical voltage signals V1 and V2 corresponding to the P1 and P2, respectively, are plotted against the range of applied temperature, as shown in Fig. 10. Also, the plot includes the response of a normalized variable (X) that related to V1 and V2 as defined by Eq. (2). It is evident from the results that the variable X is more consistent with the applied temperature with enhanced linearity coefficient of 0.9989. The slope of the line X is found to be 4.451 mV/°C with a standard error of 0.0068 V. It is also observed that X, the normalized variable is independent of source power fluctuations.

4.3 *Temperature Display*

After the interrogation of FBG sensor, the output is integrated with the display system as discussed in Sec. 2.5. The final output of the display system is plotted against the applied

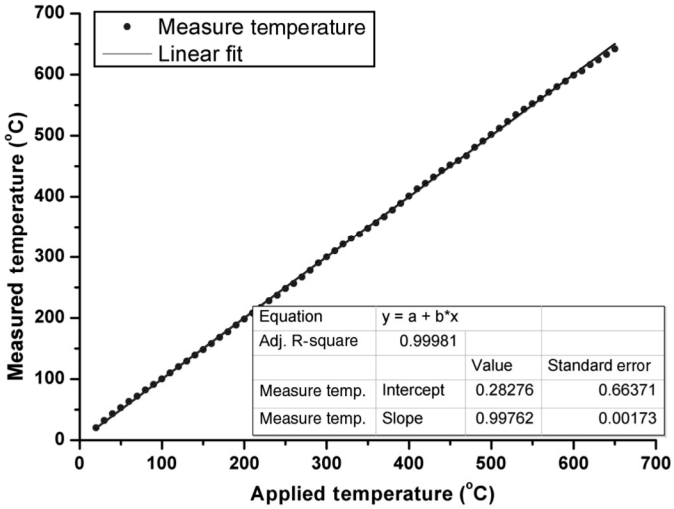

Fig. 11 Temperature display of the sensor system over the span of 20°C–650°C.

temperature as shown in Fig. 11. The sensor measured and displayed temperatures of up to 650°C with a resolution of 1°C. The experimental results revealed that the response of the system is linear with a coefficient of 0.999, and accurate with a negligible error bar of ±1.23%.

5 Conclusion

An FBG-based high-temperature sensor accompanied by a low-cost detection system has been in-house designed and successfully tested. It is evident from the test results that the sensor measures temperatures from 20°C to 650°C with a resolution of 1°C. The important aspects that are involved in this sensor system are; (1) design of a rigid sensor probe by encapsulating the bare FBG without compromising its sensitivity and response time, (2) rendering the measurement system cost-effective by employing an LPG as an edge filter to replace OSA with a simple PD, (3) rendering the sensor output independent of source power fluctuations, and (4) displaying the sensor output directly in degrees Celsius.

Acknowledgments

The authors thank the Department of Electronics and Information Technology under the Ministry of Communications and Information Technology, New Delhi, for providing financial assistance to carry out this work.

References

1. L. Michalski et al., *Temperature Measurement*, 2nd ed., John Wiley & Sons, London, pp. 397–411 (2001).
2. B. Zhang and M. Kahrizi, "High-temperature resistance fiber Bragg grating temperature sensor fabrication," *IEEE Sens. J.* **7**(4), 586–591 (2007).
3. G. Yang et al., "Real-time temperature measurement with fiber Bragg sensors in lithium batteries for safety usage," *Measurement* **46**(9), 3166–3172 (2013).
4. A. Othonos and K. Kalli, *Fiber Bragg Gratings Fundamentals and Applications in Telecommunication and Sensing*, pp. 223–388, Artech House, Boston (1999).
5. S. J. Mihailov, "Fiber Bragg grating sensors for harsh environments," *Sensors* **12**, 1898–1918 (2012).
6. R. Kashyap, *Fiber Bragg Gratings*, Academic Press, San Diego, pp. 55–85 (1999).
7. P. Fomitchov and S. Krishnaswamy, "Response of a fiber Bragg grating ultrasonic sensor," *Opt. Eng.* **42**(4), 956–963 (2003).
8. V. R. Mamidi et al., "Characterization of encapsulating material for fiber Bragg grating based temperature sensor," *Fiber Integr. Opt.* **33**(4), 325–335 (2014).
9. Y.-J. Rao, "Review article: in-fibre Bragg grating sensors," *Meas. Sci. Technol.* **8**(4), 355–375 (1997).
10. E. Al-Fakih, N. A. Abu Osman, and F. R. Mahamd Adikan, "The use of fiber Bragg grating sensors in biomechanics and rehabilitation applications: the state-of-the-art and ongoing research topics," *Sensors* **12**, 12890–12926 (2012).
11. Y. J. Rao et al., "Optical in-fiber Bragg grating sensor system for medical applications," *J. Biomed. Opt.* **3**(1), 38–44 (1998).
12. W. Du et al., "Fundamentals and applications of optical fiber Bragg grating sensors to textile structural composites," *Compos. Struct.* **42**, 217–229 (1998).
13. G. P. Brady et al., "Bragg grating temperature and strain sensors," *Proc. SPIE* **2360**, 510–513 (1994).
14. K. Srimannarayana et al., "Fiber Bragg grating and long period grating sensor for simultaneous measurement and discrimination of strain and temperature effects," *Opt. Appl.* **38**(3), 601–608 (2008).
15. A. Othonos, "Fiber Bragg gratings," *Rev. Sci. Instrum.* **68**(12), 4309 (1997).

16. V. R. Mamidi et al., "Fiber Bragg grating-based high temperature sensor and its low-cost interrogation system with enhanced resolution," *Opt. Appl.* **44**(2), 299–308 (2014).
17. V. R. Mamidi et al., "Method to athermalize a long-period fiber grating for interrogation of fiber Bragg grating–based sensors," *Opt. Eng.* **53**(9), 096111 (2014).
18. Element 14, data sheet, "Application Note Multifunctional 2-Channel Amplifier Board," http://www.farnell.com/datasheets/65044.pdf

Venkata Reddy Mamidi received his BSc degree from Osmania University, Hyderabad, India, in 2008 and his MSc (Tech.) degree in engineering physics with instrumentation specialization from the National Institute of Technology, Warangal, India, in 2011. Currently, he is pursuing his PhD at the Department of Physics, NIT, Warangal. His research interests include optical fiber sensors and their applications, electrostatics, and optoelectronic instrumentation. He is a member of SPIE and OSA.

Srimannarayana Kamineni received his BSc degree from Andhra University, Visakhapatnam, in 1971 and MSc(Tech.) and PhD degrees in engineering physics in the fields of photonics from Regional Engineering College (now NIT), Warangal, in 1974 and 1978, respectively. He joined as a faculty member in the Department of Physics, NIT Warangal, in 1977 and is currently working as a professor. His present research interests include fiber-optic sensors, passive components in telecommunications, laser metrology, and holography for NDT.

L. N. Sai Prasad Ravinuthala received his BSc degree from Sri Venkateswara University, Tirupati, India, in 1976 and his MSc degree from Andhra University, Visakhapatnam, in 1979. He completed his PhD at Regional Engineering College (now NIT), Warangal, in 1985. He joined as a faculty member in the Department of Physics, NIT Warangal, in 1986 and is currently working as a professor. His present research interests include electronic instrumentation, holographic NDT, FBG sensors, and signal processing.

Manohar Martha received his BSc degree from Kakatiya University, Warangal, India, in 2007 and MSc(Tech.) degree in engineering physics with electronics specializing from National Institute of Technology, Warangal, in 2011. He is currently working as a lecturer in Uwezo Lerning Pvt. Ltd., Hyderabad. His research interests include low-temperature sensing and fiber optic sensors.

Sai Shankar Madhuvarasu obtained his MSc(Tech.) degree in engineering physics from Regional Engineering College (now NIT), Warangal in 1977 and PhD in the field of applied optics from Kakatiya University, Warangal, in 1986. He joined as a faculty member in the Department of Physics, NIT Warangal in 1979 and is currently working as a professor. His present research interests include optical system design, optical metrology, and fiber optic sensors.

Venkatappa Rao Thumu received his BSc degree from Osmania University, Hyderabad, in 1983 and his MSc degree in physics from Kakatiya University, Warangal, in 1987. He obtained his PhD from Kakatiya University in 1994. He worked as a faculty member at Kakatiya University from 1994 to 2008. He has been working as an assistant professor at NIT Warangal, since 2008. His research interests include highly correlated electron systems, optoelectronics, fiber-optic sensing, polymer degradation, polymer blends, and spintronic materials.